Effect of Asymmetric Layout of IGBT Modules on Reliability of Motor Drive Inverters

Choi, Ui Min; Vernica, Ionut; Blaabjerg, Frede

Published in:
IEEE Transactions on Power Electronics

DOI (link to publication from Publisher):
10.1109/TPEL.2018.2828145

Publication date:
2019

Document Version
Accepted author manuscript, peer reviewed version

This article has been accepted for publication in a future issue of this journal, but has not been fully edited. Content may change prior to final publication. Citation information: DOI 10.1109/TPEL.2018.2828145, IEEE Transactions on Power Electronics

Effect of Asymmetric Layout of IGBT Modules on Reliability of Motor Drive Inverters

Ui-Min Choi, *Member, IEEE*, Ionut Vernica, *Member, IEEE*, and Frede Blaabjerg, *Fellow, IEEE*

***Abstract*—Power electronics inverters are one of major failure sources in motor drive systems and power devices are one of the main causes of the power electronics inverter failures. Typically, an IGBT module has multiple power devices due to some technical and cost advantages. This kind of configurations could have an asymmetric internal layout, which may lead to different thermal loadings and thereby lifetime difference of the power devices. Therefore, both the power rating and the lifetime of inverters are limited by the most stressed device. However, generally a common data is provided for all devices in the datasheet and this may cause improper design of the inverters in terms of the lifetime and the power rating. In this paper, an effect of an asymmetric layout of IGBT modules on the reliability of motor drive inverters is studied based on a 3-phase motor drive application with a 600 V, 30 A, 3-phase transfer molded IGBT module. The thermal impedances of 6 IGBTs are investigated and its effect on thermal loadings of power devices is studied under the given mission profile. Then, their lifetimes are estimated and compared. Finally, this effect is verified by the experiments.**

***Keywords*—Motor drives, inverter, reliability, IGBT module.**

I. Introduction

Motor drive systems have been widely used in various applications such as ship propulsion, rail traction, steel mills, water pump system, home appliance and nowadays their use has been extended to aerospace, electric vehicle and etc [1]-[2]. As roles of motor drive systems have gradually increased, the reliability of motor drive systems is getting important issue because it is very closely related to the cost aspect as well as the safety aspect. According to [3], power electronics inverters are one of major failure sources in motor drive systems and power devices are one of main causes of power electronic inverter failures [4]. Therefore, much research has been performed on the reliability of power devices such as condition monitoring, fault detection and fault-tolerant controls [5]-[10]. Further, recently, the lifetime prediction of power devices in power electronic inverters is one of major concerns and possibilities for Design for Reliability (DFR) [11]-[12].

Wire-bonded IGBT modules are one of the most widely used of their kind for various applications in a power range from several hundreds of watts (W) to several megawatts (MW) [13]. The wire-bonded IGBT module consists of different materials and it is well known that thermal stress is a main cause of package-related failures because the thermo-mechanical stress is applied to the point of contact of different materials under temperature variation due to the Coefficient Thermal Expansion (CTE) mismatch between different materials [14].

There are typically multiple power devices inside an IGBT module for some advantages [15]. However, this kind of configurations could have an asymmetric layout and thus results in thermal impedance differences among power devices. Thereby, they have different thermal loadings in real applications that might lead to discrepancy in the lifetime of the power devices. Therefore, both the lifetime and the power rating of an inverter are limited by the most stressed device. However, typically a common data for all power devices are provided in the datasheet and it causes the improper design of inverters in terms of the lifetime and the power rating.

In this paper, an effect of an asymmetric layout of IGBT modules on the reliability of power inverters is studied based on a 3-phase motor drive application using 600 V, 30 A, 3-phase transfer molded IGBT module. The thermal impedances of 6 IGBTs are investigated and its effect on the thermal loadings of the power devices is studied under the given mission profile of the motor drive system. Then, the lifetimes of power devices are estimated from the thermal loadings and compared. Finally, this effect is verified by the experiments.

II. Transfer Molded IGBT Module for Motor Drive Inverters

A. Molded power IGBT module

Transfer molded IGBT modules are widely used in low power motor drive applications such as water pumps and home appliances due to their advantages like compactness, low cost, and high reliability [16]. In the case of inverter modules for low power 3-phase motor drives, they generally consist of 6 IGBTs and 6 diodes. Such kind of configurations could have an asymmetric internal layout and thereby leads to thermal impedance differences among devices.

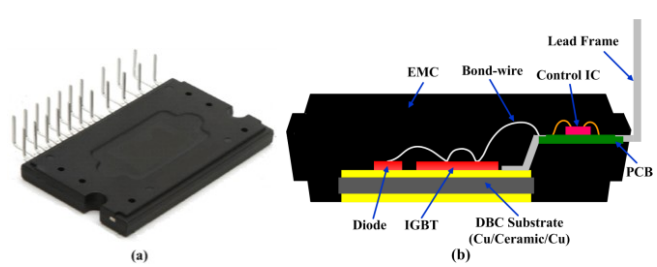

Fig. 1. Transfer molded IGBT module (a) physical appearance (b) cross section structure.

This article has been accepted for publication in a future issue of this journal, but has not been fully edited. Content may change prior to final publication. Citation information: DOI 10.1109/TPEL.2018.2828145, IEEE Transactions on Power Electronics

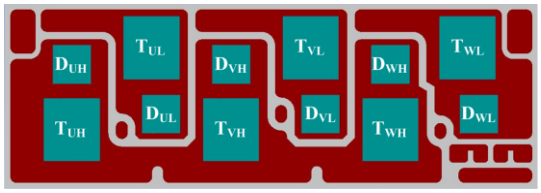

Fig. 2. Internal layout of the molded IGBT module shown in Fig. 1.

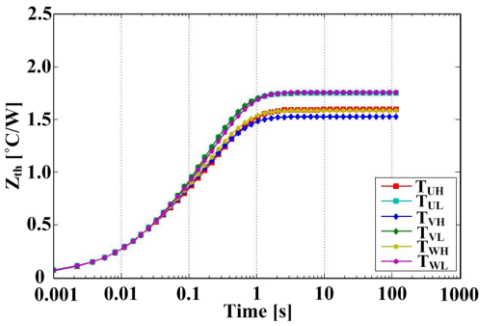

Fig. 3. Transient thermal impedances of the 6 IGBTs in the molded IGBT modules.

Fig. 1 shows one kind of transfer molded IGBT modules, which is the target IGBT module in this paper. The power rating is 600 V and 30 A and it consists of 6 IGBTs and 6 diodes. They are mounted on a Direct Bonded Copper (DBC) substrate with wire-bond interconnection. The lead frame is connected to the DBC substrate by soldering and a copper surface of the DBC substrate is exposed to be contacted with an external heat-sink. Further, gate driver circuits are embedded inside the module.

Fig. 2 shows the internal layout of the target IGBT module. This module has the asymmetric internal layout, especially between the upper group of power devices (IGBTs: $T_{XH(X=U,V,W)}$ and diodes: D_{XH}) and lower group of power devices (IGBTs: T_{XL} and diodes: D_{XL}). Thus, it can be expected that they have different thermal impedances in practice.

B. *Thermal impedances of power devices in molded power IGBT module*

Fig. 3 shows transient thermal impedances of the 6 IGBTs obtained by a Finite Element Method simulation. In this module, power losses in the IGBTs are dominant when it is used for inverters and therefore this paper is focusing on the IGBTs. Each IGBT has almost the same impedance at a short transient time, which is below 0.05 s. However, the lower group of IGBTs (T_{UL}, T_{VL}, T_{WL}) have higher thermal impedance than the upper group of IGBTs (T_{UH}, T_{VH}, T_{WH}), when the transient time is longer. Its difference is getting larger as the transient time is longer and is saturated as constant around 2 s. From this, it can be expected that a fast power loss variation by a periodical commutation of the IGBT does not affect the temperature difference among the IGBTs. However, the power loss variation at low fundamental frequencies of output or the power loss variation by load changes, which is typically in the second range or above, leads to different thermal loadings of the IGBTs and finally, it results in the lifetime difference among the IGBTs.

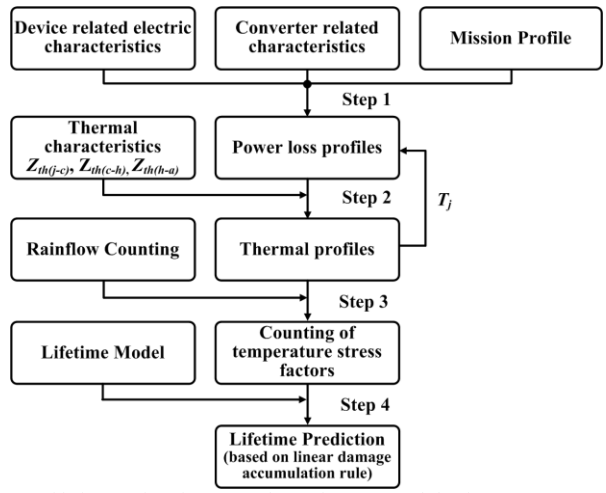

Fig. 4. Lifetime estimation procedure of IGBT modules in power converter applications [17].

III. Lifetime of Molded Power IGBT Module in Motor Drive System

In order to investigate the effect of the thermal impedance difference on the reliability of the upper and lower IGBTs, a case study is carried out with a specific mission profile of a motor application. T_{VH} and T_{VL} are considered in this case study because they have the largest thermal impedance mismatch and the thermal impedances of T_{UL}, T_{VL} and T_{WL} are almost the same. The thermal loadings of T_{VH} and T_{VL} are investigated and then the lifetimes are estimated based on their thermal loadings.

Fig. 4 shows the whole procedure to estimate lifetimes of power devices in an IGBT module [17].

In the first step, loss profiles of power devices are obtained from input data such as device characteristics, converter characteristics and mission profiles of power converter applications. Then, the loss profiles of power devices are converted to temperature profiles by thermal models of power devices. In step 3, the different temperature stress factors such as junction temperature swing (ΔT_j) and mean junction temperatures (T_{jm}) are counted from the temperature profiles by using a Rainflow counting method [18]. Finally, lifetimes of power devices in the IGBT module are predicted based on a Linear Damage Accumulation rule by putting the accounted temperature stress factors into a lifetime model, which are typically developed by power cycling tests.

A. *Motor drive system*

Fig. 5 shows a configuration of a 3-phase motor drive system with Permanent Magnet Synchronous Motor (PMSM) for the case study and related parameters for the motor drive inverter and PMSM are listed in TABLE I.

Fig. 6 shows a mission profile composed of information on torque and speed profiles. The maximum torque is 24 Nm and the maximum speed is 2000 rpm. The motor is operated for 15 s with the maximum torque and the maximum speed with 2 s ramp-up time and it is stopped for 15 s.

This article has been accepted for publication in a future issue of this journal, but has not been fully edited. Content may change prior to final publication. Citation information: DOI 10.1109/TPEL.2018.2828145, IEEE Transactions on Power Electronics

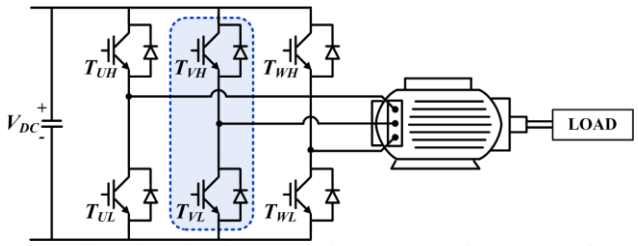

Fig. 5. Configuration of 3-phase motor drive system with PMSM for the case study.

TABLE I. PARAMETERS OF PMSM FOR THE CASE STUDY

Parameters	Symbol	Value	Unit
Nominal Power	P_n	5000	[W]
Nominal Torque	T_n	24	[Nm]
Nominal Speed	n_n	2000	[rpm]
Maximum Current	I_{max}	100	[A]
Maximum EMF	$V_{EMF,max}$	520	[V]
Rotor Inertia	J	0.0055	[Kgm^2]
Number of Pole pairs	N_{PP}	4	[-]
Stator Resistance	R_s	0.39	[Ω]
Stator Inductance	L_s	4.9	[mH]
DC-link Voltage	V_{DC}	400	V
Switching Frequency	f_{SW}	15	kHz

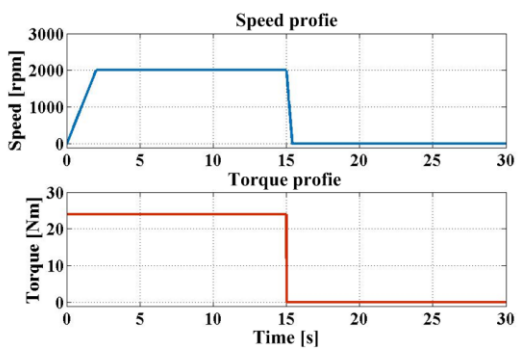

Fig. 6. Mission profile of the motor driver for the case study.

Thus, the one period of the mission profile is 30 s. This is one of typical start-run-stop processes in motor drive applications. The corresponding output currents and reference voltages of the motor drive under the given mission profile are shown in Fig. 7.

B. Power loss profiles

In order to get the thermal loadings of T_{VH} and T_{VL}, the power loss profiles of T_{VH} and T_{VL} should be obtained first.

The total power loss of the IGBT is composed of a conduction loss (P_{cond}) and a switching loss (P_{sw}).

The average conduction loss in one switching cycle can be represented as

$$P_{cond(T_H/T_L)} = V_{CE\_ON(T_H/T_L)} \cdot I \cdot d \tag{1}$$

where I is the collector current, d is the duty cycle and $V_{CE\_ON(T_H/T_L)}$ is the on-state collector-emitter voltage at the certain reference junction temperature T_H or T_L.

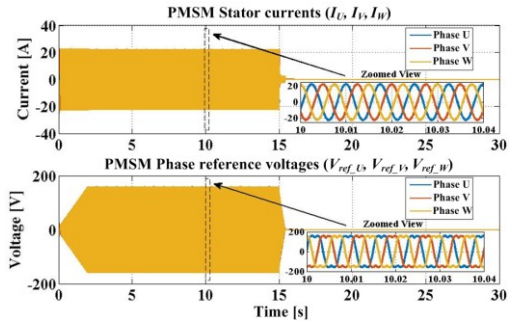

Fig. 7. The output currents and reference voltages under the given mission profile described in Fig. 6.

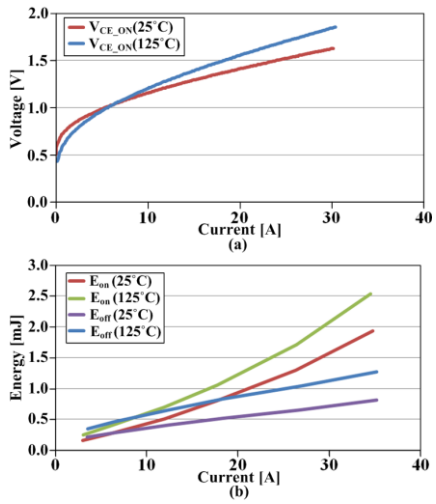

Fig. 8. V_{CE_ON} and E_{sw} of the IGBTs when the junction temperatures are 125 °C (T_H) and 25 °C (T_L).

The switching loss of the IGBT is calculated as

$$P_{sw(T_H/T_L)} = f_{sw} \cdot E_{sw} \tag{2}$$

where f_{sw} is the switching frequency and E_{sw} is the switching energy of the IGBT at the certain reference junction temperature T_H or T_L.

Fig. 8 shows V_{CE_ON} and E_{sw} of the IGBTs when the junction temperatures are 125 °C (T_H) and 25 °C (T_L), respectively. Those values can be found in the datasheet or by experiments.

It is known that both switching and conduction losses are dependent on junction temperature and thus junction temperature information of power devices should be included when power losses are calculated.

Consequently, the conduction loss and the switching loss of the IGBT at the certain junction temperature can be computed as

$$P_{cond/sw(T_j)} = \frac{P_{cond/sw(T_H)} - P_{cond/sw(T_L)}}{T_H - T_L}(T_j - T_L) + P_{cond/sw(T_L)} \tag{3}$$

Fig. 9 shows the loss profiles of T_{VH} and T_{VL} under the given mission profile shown in Fig. 6.

This article has been accepted for publication in a future issue of this journal, but has not been fully edited. Content may change prior to final publication. Citation information: DOI 10.1109/TPEL.2018.2828145, IEEE Transactions on Power Electronics

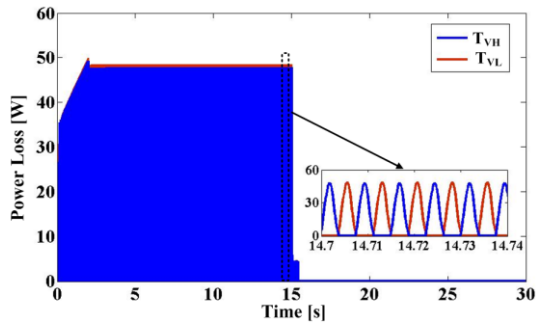

Fig. 9 Power loss profiles of T_{VH} and T_{VL} during the given mission profile (see Fig. 6).

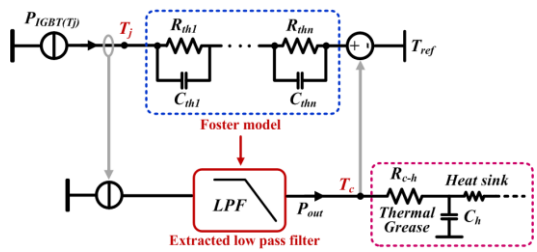

Fig. 10 Thermal impedance model for obtaining thermal loadings of the IGBTs [19].

C. Thermal profile and lifetime estimation

The thermal loading of each device can be obtained from the power loss profiles and a thermal model with thermal impedances. In this paper, the thermal model proposed in [19] are used as shown in Fig. 10 in order to translate the power loss profiles into the thermal loadings of the devices. This thermal model has two thermal paths.

The first thermal path is used for the junction temperature estimation. In this path, the multi layer RC Foster thermal network is used. The RC Foster thermal network is represented as

$$Z_{th(j-c)}(t) = \sum_{i=1}^{n} R_i (1 - e^{-t/\tau_i}) \tag{4}$$

where $Z_{th(j\text{-}c)}$ is the junction to case thermal impedance, $\tau_i = R_i * C_i$ and i means the different layers of power module for the Foster model. The related parameter can be obtained from datasheet or experiments. In this path, only the reference temperature (T_{ref}) is connected, where the T_{ref} is determined by the case temperature T_c from the other thermal path.

The second thermal path is used for the temperature estimations outside IGBT module such as case and heat-sink temperatures. In this path, the filtered power loss by a low pass filter (LPF) is used to model the loss behaviors flowing out of the device, where the parameters for the LPF can be extracted from the RC Foster thermal network in the first thermal path. The filtered loss can help to obtain correct temperature behavior outside the IGBT module.

The thermal impedances of T_{VH} and T_{VL} and the related thermal impedances for this study are listed in the TABLE II. In this simulation study, it is assumed that the heat-sink temperature is 35 ˚C.

TABLE II. JUNCTION TO CASE, CASE TO HEAT-SINK AND HEAT-SINK TO AMBIENT THERMAL IMPEDANCES

Impedance	IGBT		*i*			
			1	2	3	4
$Z_{th(j\text{-}c)}$ (Junction to case)	T_{VH}	R	0.6667	0.4060	0.3720	0.0801
		C	0.2419	0.0583	1.3502	0.0162
	T_{VL}	R	0.4221	0.8770	0.3717	0.0820
		C	1.1793	0.1937	0.0642	0.0170
$Z_{th(c\text{-}h)}$ (Case to heat-sink)	-	R	0.04132	-	-	-
		C	13.06	-	-	-

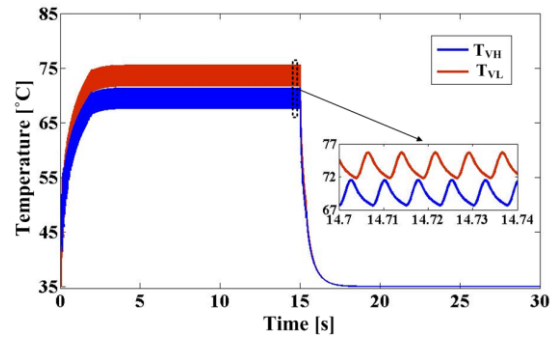

Fig. 11. Thermal loadings of T_{VH} and T_{VL} under the given mission profile of the motor drive system shown in Fig. 6.

Fig. 11 shows the thermal loadings of T_{VH} and T_{VL} under the given mission profile of the motor drive system. As expected in B of §II, both IGBTs have almost the same junction temperature swing, which is less than 4 ˚C by the periodical commutation of the IGBTs with fast output frequency as shown in the zoomed view of Fig. 11. However, they have different thermal stress in terms of junction temperature swing (ΔT_j) and mean junction temperature (T_{jm}) by the load variation. T_{VL} has a higher thermal loading compared to T_{VH} and therefore it can be expected that T_{VL} has a shorter lifetime than T_{VH}.

After the corresponding thermal loadings of T_{VH} and T_{VL} are obtained, the lifetimes of T_{VH} and T_{VL} can be estimated by mapping the thermal loadings to the lifetime model. The rainflow counting method is performed first in order to translate the thermal loading profiles of T_{VH} and T_{VL} into the number of cycles of different magnitudes of temperature stress factors such as ΔT_j and T_{jm} [16]. Then, the lifetimes are calculated based on the Linear Damage Accumulation (LDA) rule [17], [20].

In the LDA rule, if there are k different stress levels and a certain material is exposed to a i_{th} stress for a certain number of cycles n_i and the number of cycles to failure at a i_{th} stress is N_i, a damage (D) can be represented as

$$D_i = \frac{n_i}{N_i} \tag{5}$$

where n_i is the number of cycles accumulated at i_{th} stress, D_i is damage of life consumed by exposure to the cycles at i_{th} stress level.

This article has been accepted for publication in a future issue of this journal, but has not been fully edited. Content may change prior to final publication. Citation information: DOI 10.1109/TPEL.2018.2828145, IEEE Transactions on Power Electronics

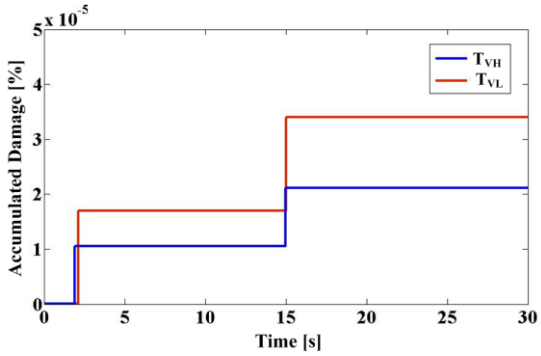

Fig. 12. Accumulated damages of T_{VH} and T_{VL} during a period of the mission profile based on the Semikron lifetime model.

The total damage at different stress levels can be added up for a total Accumulated Damage (AD) as given in (6) if different stress levels lead to the same failure mechanism.

$$AD = \sum_{i=1}^{k} \frac{n_i}{N_i} = \frac{n_1}{N_1} + \frac{n_2}{N_2} \cdots + \frac{n_{k-1}}{N_{k-1}} + \frac{n_k}{N_k} \tag{6}$$

Finally failure occurs, when a total accumulated damage is reached to 1.

In this paper, the Semikron lifetime model presented in [15] is used since there is no existing lifetime model for the target IGBT module. Therefore, the lifetime value should be considered only for the purpose of the lifetime comparison between T_{VH} and T_{VL}.

Fig. 12 shows the accumulated damage of T_{VH} and T_{VL} based on the Semikron lifetime model during a period of the mission profile.

The lifetime can simply be calculated as below

$$Lifetime = \frac{Period\ of\ mission\ profile(s)}{Operating\ time(s) * Accumulated\ damage} \tag{7}$$

If it is assumed that the motor system is operated for 12 hours per day, based on (7), the corresponding estimated lifetimes of T_{VH} and T_{VL} are about 9 years and 5.6 years, respectively. The lifetime of T_{VL} is about 38 % shorter than that of T_{VH}. In other words, the IGBTs in the lower group (T_{UL}, T_{VL}, T_{WL}) are the most reliability-critical devices and thus the lifetime of the inverter could depend on the lower group of IGBTs.

IV. Experimental Results

Experiments have been carried out in order to verify the effect of asymmetric layout of IGBT modules on the reliability of motor drive inverters.

The same IGBT module with the simulation study, which is 600 V, 30 A 3-phase transfer molded IGBT module has been used for the experiments. The IGBT module is opened as shown in Fig. 13 and painted by black paint in order to measure junction temperatures of T_{VH} and T_{VL} by high-resolution Infra-Red camera (FLIR X8400sc) when it is operated under the given mission profile of the motor drive.

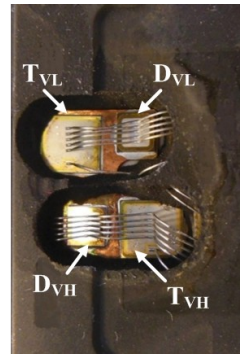

Fig. 13. Opened transfer molded IGBT module.

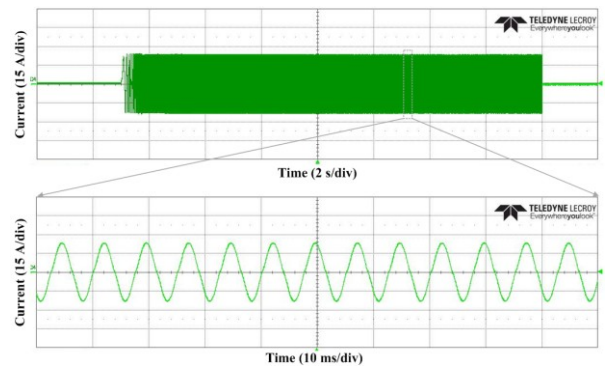

Fig. 14. Output current of phase-V during the given mission profile of the motor drive system.

Fig. 14 shows the output current of the phase-V when the motor drive inverter is operated under the given mission profile as shown in Fig. 7 and TABLE I. The heat-sink temperature is controlled by the water cooling system so that the average of the heat-sink temperature during the mission profile is kept about 35 ˚C.

Fig. 15 shows the average junction temperatures of T_{VH} and T_{VL} measured by Infra-Red camera under the given mission profile. The maximum average temperatures of T_{VL} and T_{VH} are about 73 ˚C and 68 ˚C, respectively. As expected, the thermal loading of T_{VL} is larger than that of T_{VH} in terms of junction temperature swing and the mean junction temperature due to the unbalance of the thermal impedance, which is caused by the internal asymmetric layout. Therefore, it can be expected that T_{VL} has a shorter lifetime than T_{VH}.

Fig. 16(a) and (b) show the figures of T_{VH} and T_{VL} taken by the Infra-Red camera when they have the maximum temperatures, respectively. It can be clearly seen that T_{VL} has a higher junction temperature than T_{VH}.

Furthermore, the power cycling test has been performed in order to verify that the IGBTs in the lower group (T_{UL}, T_{VL}, T_{VH}) have shorter lifetimes than the IGBTs in the upper group (T_{UL}, T_{VL}, T_{VH}). The power loading that output current (I) = 29 A_{peak}, output voltage (V_{out}) = 140 V_{peak} and output frequency (f_{out})= 1 Hz is applied to the IGBT module, where the heat-sink temperature is controlled as 25 ˚C. The reason that f_{out} is set to 1 Hz is to get the thermal loading in a second range easily by the output current and also to get the high thermal loading in order to get the test result in a reasonable testing time.

This article has been accepted for publication in a future issue of this journal, but has not been fully edited. Content may change prior to final publication. Citation information: DOI 10.1109/TPEL.2018.2828145, IEEE Transactions on Power Electronics

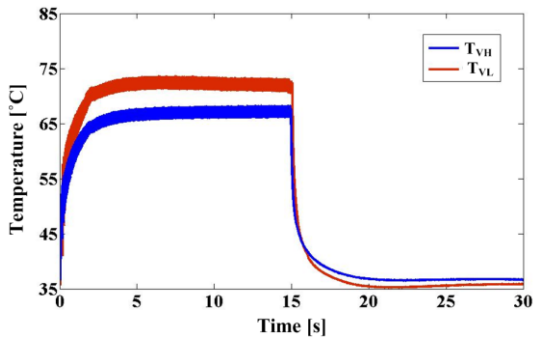

Fig. 15. Measured average junction temperatures of T_{VH} and T_{VL} by the Infra-Red camera during the mission profile.

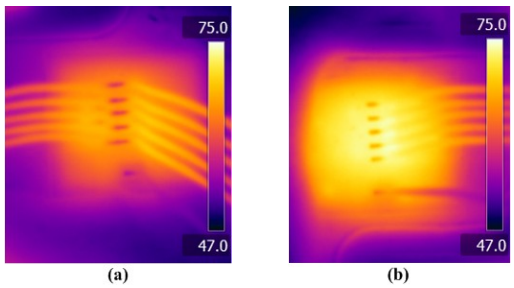

Fig. 16. Open transfer molded IGBT module taken by the Infra-Red camera at the maximum temperature (a) T_{VH} (b) T_{VL}.

The end-of-life (EOL) criterion of the IGBT module is 5 % increase of V_{CE_ON} from its initial value. V_{CE_ON} of the 6 IGBTs are measured in real-time per temperature cycle when the current is ±20 A_{peak}. More detailed information on power cycling test can be obtained in [10], [21].

Fig. 17 shows the power cycling test result of the IGBT module. As expected, V_{CE_ON} of the IGBTs in the lower group (T_{UL}, T_{VL}, T_{WL}) increases earlier where V_{CE_ON} of T_{VL} is reached to the end-of-life criterion first at about 420800 cycles. It can also be expected that the other lower IGBTs will be reached to EOL criterion soon. However, in the case of the IGBTs in the upper group (T_{UH}, T_{VH}, T_{WH}), there are no any visible increases in V_{CE_ON}.

The power cycling test with another 600 V, 30 A 3-phase transfer molded IGBT module also has been performed under the same condition as shown in Fig. V_{CE_ON} of T_{WL} is reached to the end-of-life criterion first at about 303527 cycles and it is also expected that V_{CE_ON} of T_{UL} will increase to the end-of-life criterion. On the other hand, the increases in V_{CE_ON} of the upper IGBTs (T_{UH}, T_{VH}, T_{WH}) is not observed during the power cycling test.

These two test results clearly show that the IGBTs in the upper group (T_{UH}, T_{VH}, T_{WH}) have longer lifetimes than the IGBTs in the lower group (T_{UL}, T_{VL}, T_{WL}) because the lower IGBTs have higher thermal loadings than the upper IGBTs due to the differences of the thermal impedances.

It is worth to mention that the initial V_{CE_ON} of the lower IGBTs are higher than that of the upper IGBTs. This is because the lower IGBTs have the higher internal resistance due to longer current path in this module and also higher junction temperature at the point of V_{CE_ON} measurement due to the different thermal impedance between the upper and lower IGBTs.

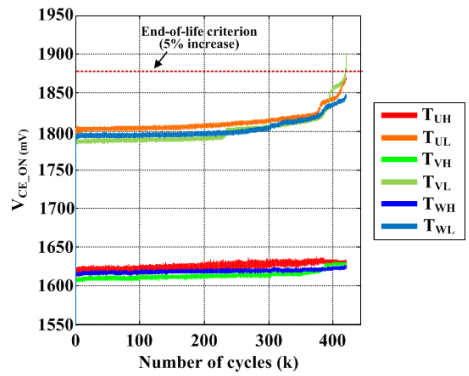

Fig. 17. Power cycling test result when output current (I) = 29 A_{peak}, output voltage (V_{out}) = 140 V_{peak} and output frequency (f_{out})= 1 Hz is applied.

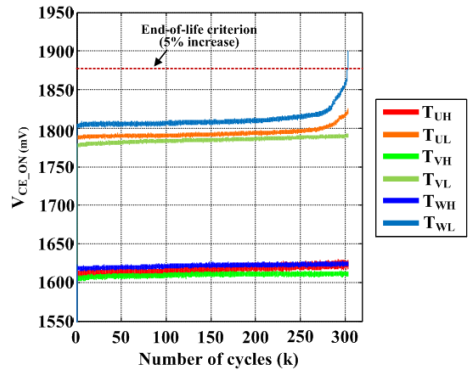

Fig. 18. Power cycling test result with another same type of the IGBT module under the same condition.

More detailed information on the internal resistance of the target IGBT module can be obtained in [22].

Furthermore, the effect of asymmetric layout of another type of IGBT module on the reliability of inverters has been validated with a small-scaled Modular Multilevel Converter (MMC). A full-bridge IGBT module manufactured by Infineon (F4-50R12KS4) is used for a sub-module of the MMC. Junction temperatures of upper and lower IGBTs of one leg in the full-bridge IGBT module are measured. In this paper, the sub-module of the MMC is operated under the following conditions; DC-link voltage (V_{DC}): 100 V, output current (I) = 40 A_{peak}, modulation index = 0.8, switching frequency (f_{SW}) = 2 kHz and output frequency (f_{out})= 50 Hz. The upper IGBT is represented as S_1 and the lower IGBT is denoted as S_2.

Fig. 19 shows the average junction temperatures of S_1 and S_2 measured by the Infra-Red camera for 120 s. The junction temperatures of S_1 and S_2 increase continuously because the heat-sink temperature is not under the steady-state condition. However, it can be clearly seen that S_1 has a higher junction temperature than S_2 due to the different thermal impedance caused by the asymmetric layout of the IGBT module. Therefore, they have the different thermal loadings in real applications and thus it can be expected that S_1 has a shorter lifetime than S_2.

Fig. 20(a) and (b) show the figures of S_1 and S_2 taken by the Infra-Red camera when they have the maximum temperatures, respectively. It can be clearly seen that S_1 has a higher junction temperature than S_2.

This article has been accepted for publication in a future issue of this journal, but has not been fully edited. Content may change prior to final publication. Citation information: DOI 10.1109/TPEL.2018.2828145, IEEE Transactions on Power Electronics

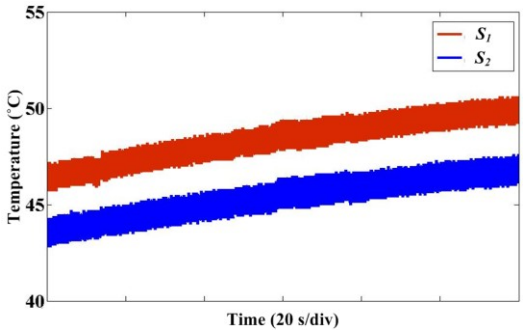

Fig. 19. Measured average junction temperatures of S_1 and S_2 by the Infra-Red camera under the MMC operation.

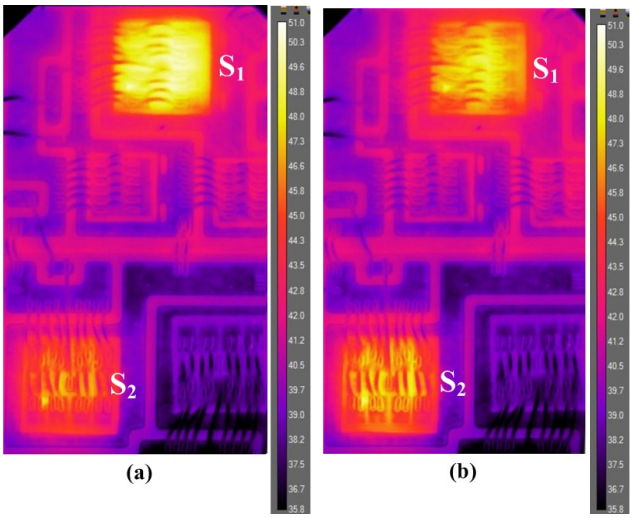

Fig. 20. Open full-bridge IGBT module taken by the Infra-Red camera at the maximum temperature of (a) upper IGBT S_1 (b) lower IGBT S_2.

V. Conclusion

In this paper, an effect of asymmetric layout of IGBT modules on the reliability of power inverters has been studied. This study has been performed with 600 V, 30 A, 3-phase molded IGBT modules under the 3-phase motor drive application.

Due to the asymmetric internal layout of the IGBT module, the 6 IGBTs have the different thermal impedances and especially the lower IGBTs have higher thermal impedances than the upper IGBTs. Because of this, the IGBTs have the different thermal loadings under the given mission profiles of the motor drive application and finally leads to mismatched lifetimes. The lifetime of T_{VL} is shorter about 38 %, which is 5.6 years than that of T_{VH}, which is 9 years. Consequently, the lower IGBTs (T_{UL}, T_{VL}, T_{VH}) are the most reliability-critical devices. Thus, the lifetime and the power rating of the inverter may be limited by the lower group of the IGBTs. However, generally a common data is provided for all devices in datasheet and this may cause improper design of the inverter in terms of the lifetime and the power rating.

This effect has been verified by the experiments. As expected, the lower IGBTs have higher thermal loadings than the upper IGBTs and therefore have shorter lifetimes.

Furthermore, this effect has also been validated with the full-bridge IGBT module in the sub-module of the small-scaled Modular Multilevel Converter. Due to the asymmetric layout of the IGBT module, the upper and lower IGBTs in one leg also have different junction temperatures. From above result, it can be expected that other kinds of IGBT modules can have an asymmetric internal layout and therefore, they can affect the reliability of inverters for other different power electronic applications such as PV inverter, wind turbine converter, electric vehicle and so on.

This study can provide a feedback to module designers on optimizing module's internal geometry such as a layout of a DBC so that power devices in power modules have thermal impedances as similar as possible for even lifetime distributions. Further, it can also give suggestions for application engineers when inverter is designed with the target lifetime and the power rating.

Reference

[1] P. Davari, Y. Yang, F. Zare, and F. Blaabjerg, "Multipulse Pattern Modulation Scheme for Harmonic Mitigation in Three-Phase Multimotor Drives," *IEEE Journal of Emerging and Selected Topics in Power Electronics*, vol. 4, no. 1, pp. 174-185, Mar. 2016.

[2] I. Boldea, "Electric Generators and Motors: an overview," *CES Transactions on Electrical Machines and Systems*, vol. 1, no. 1, pp. 3-14, Mar. 2017.

[3] K. J. P. Mackent, I.T. Wallace, and M.H.J. Bolleno, "Reliability Assessment of Motor Drives," *in Conf. Rec. PESC 2006*, pp. 1-7, June 2006.

[4] S. Yang, A. Bryant, P. Mawby, D. Xiang, L. Ran, and P. Tavner, "An Industry-Based Survey of Reliability in Power Electronic Converters," *IEEE Transactions on Industry Applications*, vol. 47, no. 3, pp. 1441-1451, May/June 2011.

[5] U. M. Choi, F. Blaabjerg, S. Jørgensen, S. Munk-Nielsen, and B. Rannestad, "Reliability Improvement of Power Converters by Means of Condition Monitoring of IGBT Modules," *IEEE Transactions on Power Electronics*, vol. 32, no. 10, pp. 7990-7997, Oct. 2017.

[6] W. Zhang, D. Xu. P. N. Enjeti, H. Li, J. T. Hawke, and H. S. Krishnamoorthy, "Survey on Fault-Tolerant Techniques for Power Electronic Converters," *IEEE Transactions on Power Electronics*, vol. 29, no. 12, pp. 6319-6331, Dec. 2014.

[7] U. M. Choi, F. Blaabjerg, and K. B. Lee, "Reliability Improvement of a T-Type Three-Level Inverter With Fault-Tolerant Control Strategy," *IEEE Transactions on Power Electronics*, vol.30, no. 5, pp. 2660-2673, May 2015.

[8] B. A. Welchko, T. A. Lipo, T. M. Jahns, and S. E. Schulz, "Fault Tolerant Three-Phase AC Motor Drive Topologies: A Comparison of Features, Cost, and Limitations," *IEEE Transactions on Power Electronics*, vol. 19, no. 4, pp. 1108-1116, July 2004.

[9] U. M. Choi, F. Blaabjerg, S. Jørgensen, F. Iannuzzo, H. Wang, C. Uhrenfeldt, and S. Munk-Nielsen, "Power cycling test and failure analysis of molded Intelligent Power IGBT Module under different temperature swing durations," *Microelectronics Reliability*, vol. 64, pp. 403-408, Sep. 2016.

[10] U. M. Choi, F. Blaabjerg, and S. Jørgensen, "Power Cycling Test Methods for Reliability Assessment of Power Device Modules in respect to Temperature Stress," *IEEE Transactions on Power Electronics*, vol. 33, no. 3, pp. 2531-2551, Mar. 2018.

[11] K. Ma, H. Wang, and F. Blaabjerg, "New Approaches to Reliability Assessment: Using physics-of-failure for prediction and design in power electronics systems," *IEEE Power Electronics Magazine*, vol. 3, no. 4, pp. 28-41, Dec. 2016.

[12] D. Zhou, H. Wang, and F. Blaabjerg, "Mission Profile based System-level Reliability Analysis of DC/DC Converters for a Backup Power Application," *IEEE Transactions on Power Electronics*, to be published.

[13] A. Volke, and M. Hornkamp, IGBT Modules - Technologies, Driver and Application, Infineon Technologies AG, 2011. ISBN: 978-3-00-032076-7.

[14] M. Ciappa, "Selected failure mechanism of modern power modules," *Microelectronics Reliability*, vol. 42, nos. 4-5, pp. 653-667, Apr.-May 2002.

[15] A. Wintrich, U. Nicolai, W. Tursky, and T. Reimann, Application Manual Power Semiconductors, SEMIKRON International GmbH, 2011. ISBN: 978-3-938843-66-6.

[16] Y. Wang, K. Yamaguchi, K. Watabe, T. Tanaka, M. Rogers, and E. R. Motto, "A new multi-functional compact IPM for low power industrial application," *in Conf. Rec. APEC 2017*, pp. 3072 - 3075, Mar. 2017.

[17] U. M. Choi, K. Ma, and F. Blaabjerg, "Validation of Lifetime Prediction of IGBT Modules Based on Linear Damage Accumulation by Means of Superimposed Power Cycling Tests," *IEEE Transactions on Industrial Electronics,* vol. 65, no. 4, pp. 3520-3529, Apr. 2018.

[18] L. R. GopiReddy, L. M. Tolbert, B. Ozpineci, and J. O. P. Pinto, "Rainflow Algorithm-Based Lifetime Estimation of Power Semiconductors in Utility Applications," *IEEE Transactions on Industry Applications*, vol. 51, no. 4, pp. 3368-3375, July/Aug. 2015.

[19] K. Ma, N. He, M. Liserre, and F. Blaabjerg, "Frequency-Domain Thermal Modeling and Characterization of Power Semiconductor Devices," *IEEE Transactions on Power Electronics*, vol. 31, no. 10, pp. 7183-7193, Oct. 2016.

[20] J. A. Bannantine, J. J. Comer, and J. L. Handrock, Fundamentals of Metal Fatigue Analysis. Englewood Cliffs, NJ, USA: Prentice-Hall, 1990.

[21] U. M. Choi, S. Jørgensen, and F. Blaabjerg, "Advanced Accelerated Power Cycling Test for Reliability Investigation of Power Device Modules," *IEEE Transactions on Power Electronics*, vol. 31, no. 12, pp. 8371-8386, Dec. 2016.

[22] U. M. Choi, F. Blaabjerg, F. Iannuzzo, and S. Jørgensen, "Junction temperature estimation method for a 600 V, 30A IGBT module during converter operation," *Microelectronics Reliability*, vol. 55, no. 9-10, pp. 2022-2026, Aug.-Sep. 2015.